Calorimetric, dielectric, infrared spectra and thermal expansion studies of structural phase transitions in $((CH_3)_2CHNH_3)_2MX_5$ (M=Sb, Bi; X=Cl, Br) crystals

1995 J. Phys.: Condens. Matter 7 5335

(http://iopscience.iop.org/0953-8984/7/27/018)

J. Phys.: Condens. Matter 7 (1995) 5335–5350. Printed in the UK

Calorimetric, dielectric, infrared spectra and thermal expansion studies of structural phase transitions in $[(CH_3)_2CHNH_3]_2MX_5$ (M = Sb, Bi; X = Cl, Br) crystals

R Jakubas†, G Bator†, P Ciąpała†, J Zaleski‡, J Baran§ and J Lefebvre‖

† Institute of Chemistry, University of Wrocław, F Joliot Curie 14, 50-383 Wrocław, Poland
‡ Institute of Chemistry, University of Opole, Oleska 48, 45-951 Opole, Poland
§ Institute of Low Temperature and Structure Research of the Polish Academy of Science, Okólna 2, 50-422 Wrocław, Poland
‖ Laboratoire de Dynamique et Structures des Matériaux Moléculaires (UA No 801), UFR de Physique, Université de Lille I, 59655 Villeneuve d'Ascq Cédex, France

Received 19 December 1994, in final form 16 March 1995

Abstract. Differential scanning calorimetric, thermal expansion, dielectric dispersion, infrared and preliminary x-ray diffraction studies on $[(CH_3)_2CHNH_3]_2MX_5$ (M = Sb, Bi; X = Cl, Br) crystals are reported. All the studied salts are isomorphous, crystallizing in monoclinic symmetry. They undergo low-temperature structural phase transitions of first- and second-order type: $[(CH_3)_2CHNH_3]_2SbBr_5$ at 171 and 180 K, $[(CH_3)_2CHNH_3]_2BiCl_5$ at 164 K, $[(CH_3)_2CHNH_3]_2BiBr_5$ at 155 and 133 K. Dielectric dispersion studies in all isopropylammonium crystals between 100 Hz and 1 MHz reveal a low-frequency relaxation process described by the Cole–Cole formula with $\alpha \simeq 0.15$–0.20 in the phase transition temperature region. All phase transitions are likely to be due to the motion of the isopropylammonium cations.

1. Introduction

The alkylammonium halogenoantimonates(III) and bismuthates(III) crystallize in a number of different stoichiometries, of which the most popular are: RMX_4, R_2MX_5, $R_3M_2X_9$ and R_3MX_6 ($R = NH_{4-n}(CH_3)_n$); M = Sb, Bi; X = Cl, Br, I). They are ionic-molecular salts. They crystallize in anionic sublattices built of MX_6^{3-} distorted octahedra, isolated or connected with each other by bridging halogen atoms.

Recently the physical properties of the $R_3M_2X_9$ subgroup of the family have attracted considerable attention. Many compounds of this subfamily show interesting ferroic properties [1–4]. They possess a rich sequence of phase transitions, some of them to polar phases. The structural phase transitions encountered in these crystals are related to the ordering of the alkylammonium cations [5–10].

Knowledge of the physical properties of the R_2MX_5 subgroup is only fragmentary. Very recently, nuclear quadrupole resonance (NQR), differential thermal analysis (DTA) and nuclear magnetic resonance (NMR) studies of $(C_2H_5NH_3)_2SbBr_5$ have shown that it undergoes a phase transition at 155 K. It is considered to be due to the motion of the ethylammonium cation around its long axis [11]. In $(n\text{-}C_3H_7NH_3)_2SbBr_5$ a complex sequence of phase transitions, with at least six solid phases was found between 100 and 400 K [11, 12]. ^1H nuclear magnetic resonance studies on this complex showed that in the temperature range

0953-8984/95/275335+16$19.50

80–284 K the CH_3 and NH_3 groups undergo C_3 reorientation followed by cationic tumbling at higher temperature [13].

We decided to extend the studies of those derivatives in which the n-alkylammonium cations were substituted by isopropylammonium ones. As the isopropylammonium cations possess higher symmetry than that of n-propylammonium, we expect that some types of reorientation of cations occur at room temperature, which could be frozen on cooling, giving a contribution to the possible phase transitions at lower temperatures.

The goal of the present work is to synthesize the $[(CH_3)_2CHNH_3]_2MX_5$ crystals, to study the dielectric properties and phase transitions by differential scanning calorimetry (DSC), dilatometric, dielectric and infrared (IR) methods.

2. Experimental details

$[(CH_3)_2CHNH_3]_2MX_5$ were obtained in the reaction of Sb_2O_3 or $(BiO)_2CO_3$ and isopropylamine in concentrated hydrobromic or hydrochloric acid in molar ratio of 4:1. Large single crystals were obtained by slow evaporation of a saturated aqueous solution at room temperature. The stoichiometry was confirmed by elemental analysis:

(i) $[(CH_3)_2CHNH_3]_2BiCl_5$ (IPCB), C 14.10% (calc. 14.23%), N 5.50% (calc. 5.53%), H 4.01% (calc. 3.98%);

(ii) $[(CH_3)_2CHNH_3]_2SbBr_5$ (IPBA), C 11.17% (calc. 11.23%), N 4.34% (calc. 4.37%), H 3.17% (calc. 3.14%);

(iii) $[(CH_3)_2CHNH_3]_2BiBr$ (IPBB), C 9.75% (calc. 9.89%), N 3.79% (calc. 3.84%), H 2.80% (calc. 2.77%).

Complex permittivity ε^* was measured using an HP 4284A precision LCR meter from 100 Hz to 1 MHz in the temperature range between 100 and 300 K at a cooling rate of 0.2 K min^{-1}.

Calorimetric measurements were performed on a Perkin-Elmer DSC-7 differential scanning calorimeter at a scanning speed 3–5 K min^{-1} on cooling/heating.

The linear thermal expansion was measured using a dilatometer of the difference transformer type (Perkin-Elmer TMS-2 thermomechanical analyser). Under dynamic temperature conditions the measurements were performed on heating/cooling at rates of 0.1–0.5 K min^{-1}. The results were reproducible within 10–15%. The accuracy of the thermal expansion determination is about 2%.

Samples for dielectric dispersion and thermal expansion measurements were typically of size $6 \times 6 \times 1$ mm^3 and $4 \times 4 \times 4$ mm^3, respectively.

Infrared spectra of IPBA (in Nujol) in the temperature range 13–300 K were recorded with a Bruker IFS-88 Fourier-transform infrared (FT IR) spectrometer with resolution 2 cm^{-1}. An APD Cryogenics closed cycle helium cryodyne system was used for temperature-dependence studies. The temperature of the sample was maintained at an accuracy of ± 0.1 K.

The lattice parameters were refined from setting angles of 25–50 reflections in the $17 < 2\theta < 30$ range using a KM4 diffractometer and Cu K_α radiation.

3. Results

3.1. X-ray studies

Shown in table 1 are the values of the lattice parameters of isopropylammonium salts. They crystallize at room temperature in monoclinic symmetry. The similar values of the lattice

Table 1. The lattice parameters of IPCB, IPBA and IPBB crystals at room temperature.

	a (Å)	b (Å)	c (Å)	β (deg)	d_{calc} (g cm^{-3})	d_{exp} (g cm^{-3})	Z
IPCB	11.891(5)	12.740(7)	12.071(6)	114.07(4)	2.01	2.01(1)	4
IPBA	12.013(3)	12.134(5)	12.525(3)	115.26(4)	2.37	2.37(1)	4
IPBB	12.040(4)	13.244(4)	12.563(6)	115.19(4)	2.67	2.67(1)	4

parameters suggest that they are isomorphous. Weissenberg photographs were taken for IPCB crystals. From systematic absences, $P2_1/c$ group follows.

3.2. *Dilatometric studies*

The temperature dependence of the linear thermal expansion, $\Delta L/L$, measured along the a and b axes for $[(CH_3)_2CHNH_3]_2BiCl_5$ (IPCB) is shown in figure 1. Along the a axis a small positive jump in dilatation of the order 2×10^{-4} is observed at 164 K (on heating), whereas for the b axis one can only see a change in the thermal expansion coefficients (the mean value of $\overline{\alpha}$ is defined as $(\Delta L_1 - \Delta L_2)/L_{0(300\ K)}(T_1 - T_2)$), where $\overline{\alpha}_b \simeq 3 \times 10^{-5}$ K^{-1} and $\overline{\alpha}_b \simeq 5.8 \times 10^{-5}$ K^{-1} above and below 164 K, respectively. The $\overline{\alpha}_a$ coefficient in the same temperature range is distinctly larger than that observed for the b axis ($\sim 10^{-4}$ K^{-1}). The clear anomaly in the thermal expansion at 164 K of IPCB (temperature hysteresis of about 3 K) indicates the existence of a structural phase transition of slightly first- or second-order type.

The thermal dilatation of $[(CH_3)_2CHNH_3]_2SbBr_5$ (IPBA) crystals in the temperature range 165–185 K is shown in figure 2. This analogue exhibits a clear thermal anomaly at 171 K (on heating), with temperature hysteresis of about 4 K, related to the structural phase transition of first-order type. This transition is accompanied by a positive jump in length ($\Delta L/L$) of the samples of about 4.4×10^{-4} and 8×10^{-5} along the a and b axis, respectively. We should also notice a subtle anomaly in the thermal dilatation at about 180 K (with no temperature hysteresis), which could indicate a continuous phase transition (compare also DSC results presented in figure 4). The mean value of thermal expansion coefficient, $\overline{\alpha}_b$, in the studied temperature range amounts to 2×10^{-4} K^{-1} and 0.5×10^{-4} K^{-1} along the a and b axis, respectively. The temperature characteristic of the $\Delta L/L$ curve for the c axis is comparable to those obtained for the b axis in both IPCB and IPBA crystals and it is not shown in the figures.

In figure 3 the temperature dependence of the linear thermal expansion, $\Delta L/L$, of $[(CH_3)_2CHNH_3]_2BiBr_5$ (IPBB) measured along the a, b and c axes, on heating, is presented. The IPBB crystal exhibits a distinct anisotropy in thermal expansion in the studied temperature range of 110–180 K. At 155 K a clear anomaly, as a change in slope of the linear part of the $\Delta L/L$ curve, is visible along the a and b axes, whereas for the c axis a sudden change in the sign of linear expansion coefficient takes place at this point. At lower temperatures one can observe a second weak anomaly in the vicinity of 133 K. It is clear that both continuous anomalies in the thermal expansion curve in IPBB correspond to the weak second-order phase transitions confirmed by DSC measurements. These anomalies were well reproducible, on cooling, with no temperature hysteresis.

3.3. *DSC studies*

The temperature dependences of the heat flow obtained between 120 and 190 K in IPCB, IPBA and IPBB are shown in figure 4. The existence of the peak around 163 K (on cooling recorded at 161 K) corroborates the non-continuous phase transition visible in the thermal

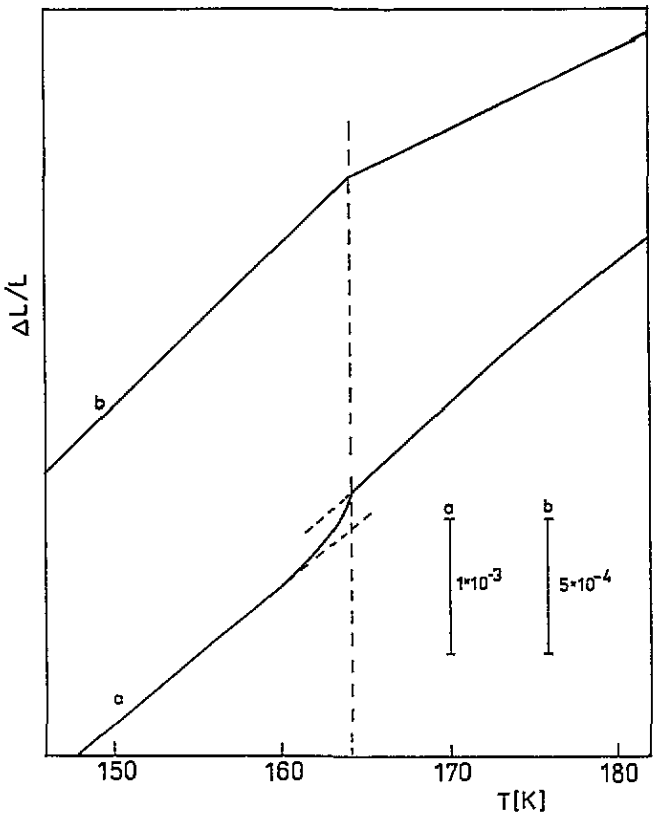

Figure 1. Temperature dependence of the linear thermal expansion, $\Delta L/L$, measured along the a and b axes for IPCB crystal, on heating.

expansion at 164 K for IPCB. It should also be noted that the thermal effect is rather small for this crystal. The DSC plot of IPBA crystal revealed two perfectly reproducible endotherms: one as a strong peak with onset at 172 K, and the other at higher temperature of about 182 K corresponding to the structural phase transition found in dilatometric measurements at 171 and 180 K. During the cooling scan of IPBA, these two peaks are better separated. The higher-temperature peak anomaly with relatively small temperature hysteresis ($\Delta T < 0.5$ K) suggests the second- or weak first-order nature of this transition and is in agreement with our dilatometric results. The DSC curve for IPBB (on heating) displays a change in slope at 133 K and at about 155 K, which was well reproducible, on cooling, with no temperature hysteresis. These two anomalies corroborate the continuous nature of structural phase transitions found in the dilatometric measurements of IPBB.

The sequence of phase transitions, the entropy effects and the changes of linear thermal expansion (for the first-order phase transition) in isopropylammonium crystals are presented in table 2. The pressure coefficients were estimated from the Clausius–Clapeyron relation $dT_c/dp = \Delta V/\Delta S$, where ΔV is the change in molar volume and ΔS is the value of the transition entropy.

3.4. IR spectra of $[(CH_3)_2CHNH_3]_2SbBr_5$

Infrared spectra of IPBA in the frequency range 4000–400 cm^{-1} at two temperatures (13 and 300 K) are presented in figure 5. The spectra in the frequency range 3000–2700 cm^{-1} are

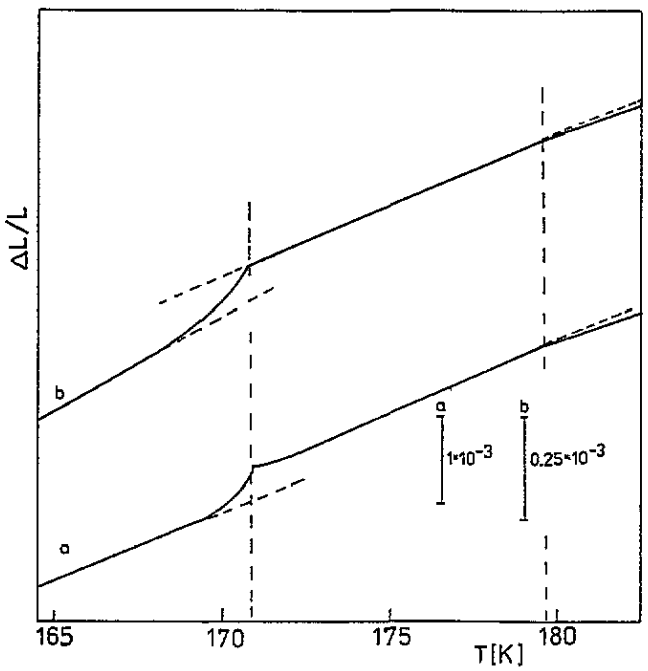

Figure 2. Thermal dilatation of IPBA crystals measured along the *a* and *b* axes in the temperature range 165–185 K, on heating.

not shown because of strong overlapping of C–H stretching modes from the IPBA crystal as well as from Nujol (broken line in figure 5). Listing of the internal mode frequencies of isopropylammonium cation for two temperatures (300 and 13 K) is given in table 3. The assignments of Hamada [15] for isopropylamine were used as guides.

Figure 6 shows the temperature dependences of the frequencies for the $\rho(NH_3^+$ rocking) mode and for the ν_a(CCC) (ν_{15}), ν(CN stretching) (ν_{13}) and $\rho(CH_3$ rocking) (ν_{29}) modes. The temperature dependences of the $\omega(NH_3^+$ wagging) (ν_{14}) and ν_s(CCC) (ν_{15}) mode frequencies are presented in figure 7.

The evolution of the infrared spectrum in the frequency region that is related to the internal modes of isopropylammonium cation show visible changes in the vicinity of the phase transition temperature (T_c = 172 K) only in the case of the $\nu_{s,a}$(CCC) (ν_{15}), ν(CN) (ν_{13}) and $\omega(NH_3^+$ wagging) (ν_{14}) modes. The low-frequency component of ν_{14} mode splits most likely into three components in the vicinity of the phase transition. In the case of the ν_s(CCC) (ν_{15}) mode, a change in the temperature coefficient of the upper frequency component and a change in the position of the lower frequency component is observed at the phase transition point. Moreover, in the low-temperature phase the new component of ν_{15} mode appears.

No drastic changes are observed for $\rho(NH_3^+)$ and for ν(CN) modes in the vicinity of the phase transition (figure 6). Nevertheless, four components of $\rho(NH_3^+)$ and nine components of ν(CN) (ν_{13}) appear in the spectra of the low-temperature phase, at about 30 K below T_c, in comparison to two and three components, respectively, at room temperature.

The components of the $\nu(NH_3^+$ stretching) mode, symmetric and antisymmetric, and $\delta(NH_3^+$ bending) (ν_6) mode (not presented in the figures) are not temperature-dependent and they are not sensitive to the phase transition.

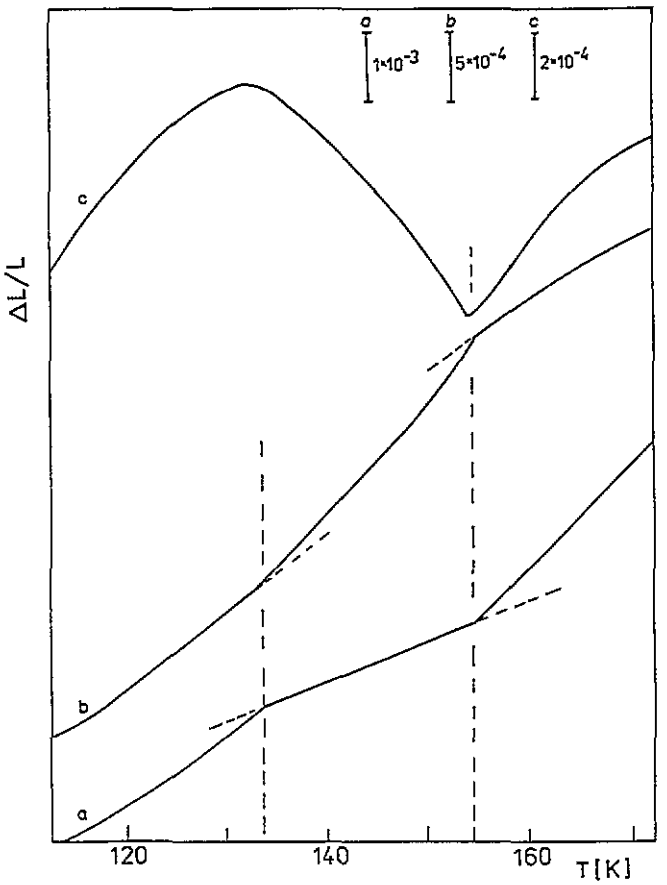

Figure 3. Thermal dilatation of IPBB crystals measured along the *a*, *b* and *c* axes in the temperature range 115–165 K, on heating.

All these changes in the IR spectra in the vicinity of the phase transition of the IPBA crystal are less distinct than in case of other alkylammonium derivatives [3].

3.5. Dielectric dispersion

The static permittivity ε_0 for IPBB, IPCB and IPBA, parallel to the *b* axis at room temperature, is equal to 12.8, 13.6 and 12.8, respectively. On lowering the temperature, $\varepsilon_{0,b}$ increases slightly and below the phase transition temperature for all crystals it drops to a value 2–3 units lower. For all the studied compounds, anisotropy of dielectric properties is found. The highest value of ε_0 is observed parallel to the *b* axis, and the lowest value parallel to the *a* axis (perpendicular to the *bc* cleavage plane). For example, in the case of IPCB the increment of permittivity $\Delta\varepsilon = \varepsilon_{\text{high-temp. phase}} - \varepsilon_{\text{low-temp. phase}}$ is equal to 2.5 and 0.2, along the *b* and *a* axis, respectively.

All the crystals (IPBB, IPCB and IPBA) in this paper show dielectric dispersion in the frequency range between 400 Hz and 1 MHz. Figures 8, 9 and 10 present the temperature dependence of real (ε') and imaginary (ε'') parts of the permittivity for some frequencies parallel to the *b*, *c* and *a* axis, respectively, for the IPCB crystal. The similar dependences for the IPBA crystal along the *a* axis are presented in figure 11. The presented dielectric

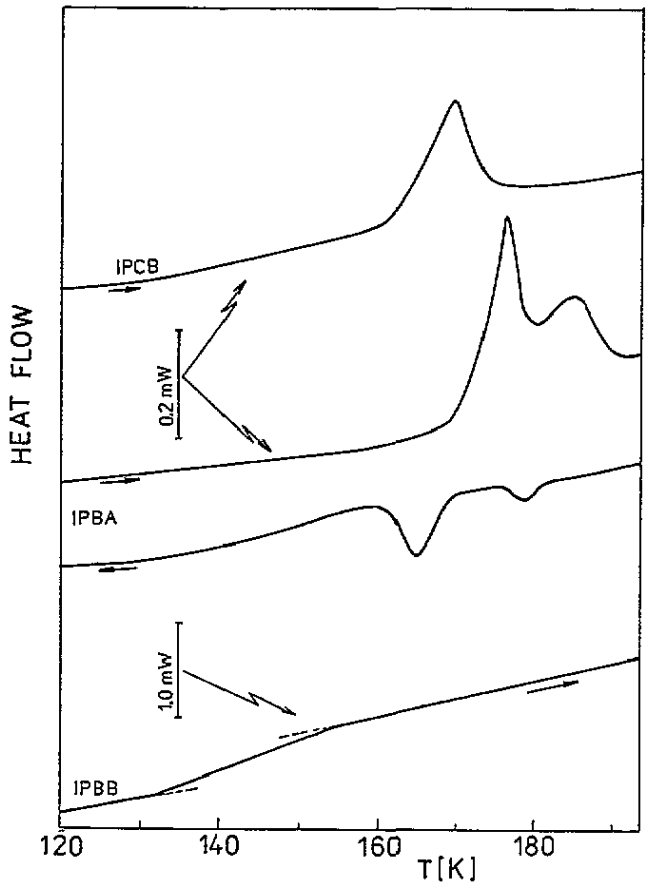

Figure 4. Heat flow in the temperature range between 120 and 190 K for the IPCB, IPBA and IPBB crystals.

Table 2. The transition temperatures, entropies, changes of transition volume and pressure coefficient dT_c/dp for isopropylammonium crystals.

	T_c^a (K)	Character of PT	ΔS (J K^{-1} mol^{-1})	$10^3\Delta V/V$	dT_c/dp (10^{-2} K MPa^{-1})
IPCB	164	First order	1.01	+0.2	+1.2
IPBA	171	First order	0.8	+0.56	+4.5
	180	Higher than first order	~0.3	—	—
IPBB	155	Second order or higher	—	—	—
	133	Second order or higher	—	—	—

[a] T_c values taken on heating, from the dilatometric studies.

response is characteristic of a crystal where gradual freezing of the rotational motion of the alkylammonium cations is observed: the higher the frequency, the higher is the temperature

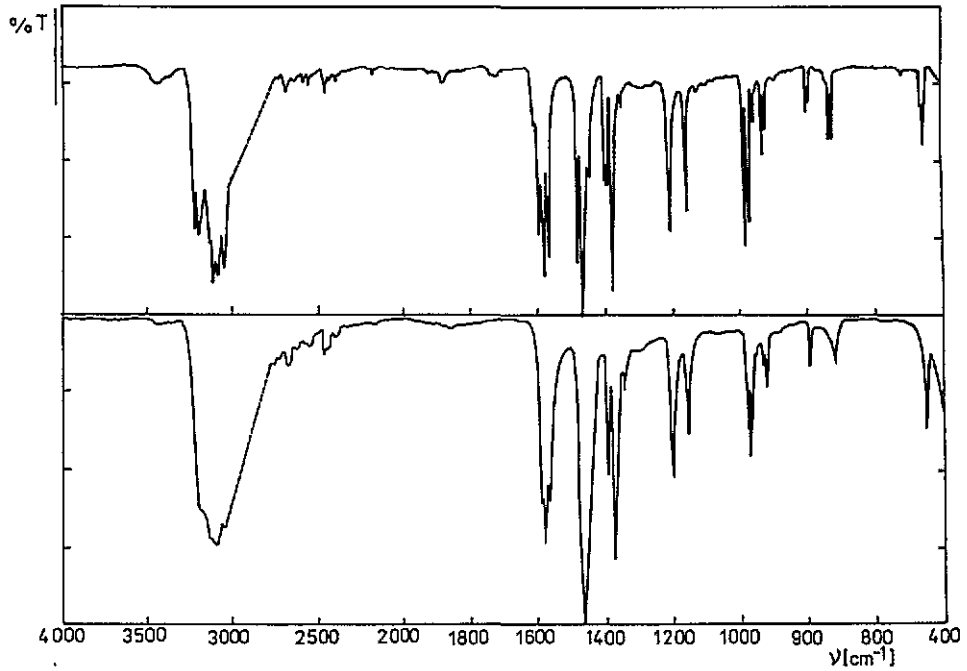

Figure 5. Infrared spectra of IPBA in the frequency range 4000–400 cm^{-1} at 13 (upper part) and 300 K (lower part).

at which a decrease of ε' takes place; the maxima of the imaginary (ε'') part also shift to higher temperature with frequency.

Dielectric measurements performed along both the c and b axes for the IPBA crystal in the phase transition region ($T_c = 168$ and 182.5 K, on cooling) did not reveal any anomaly in the $\varepsilon'(T)$ curves, whereas a small jump of ε' just below the lower-temperature phase transition is observed along the a axis. The higher-temperature structural phase transition for this crystal at 182.5 K is inactive in the dielectric studies for all crystallographic axes.

Figure 12 shows typical Cole–Cole diagrams at five temperatures (228, 218, 210, 193 and 186 K) for the IPCB crystal. The temperature dependence of the macroscopic relaxation time ($\tau(T)$) was obtained by the best fit of the Cole–Cole function:

$$\varepsilon' - i\varepsilon'' = \varepsilon_\infty + \frac{\varepsilon_0 - \varepsilon_\infty}{1 + [i\omega\tau(T)]^{1-\alpha}}. \tag{1}$$

The temperature dependence of relaxation times for IPBB, IPCB and IPBA is presented in figure 13. The macroscopic relaxation time τ of reorientation of the non-interacting dipoles is given by [14]

$$\tau = C\exp(\Delta E^{\ddagger}/k_B T) \tag{2}$$

where $\Delta E^{\ddagger}$ represents the potential barrier height of dipole reorientation and C = constant. It is seen from figure 12 that τ is well fitted by formula (2) where $\Delta E^{\ddagger}$ was estimated to be $\sim$ 0.30 eV (4.32×10^{-20} J) for all studied crystals. Therefore, it may be suggested that dipole–dipole interaction is negligible in the mechanism of the phase transition in isopropylammonium crystals.

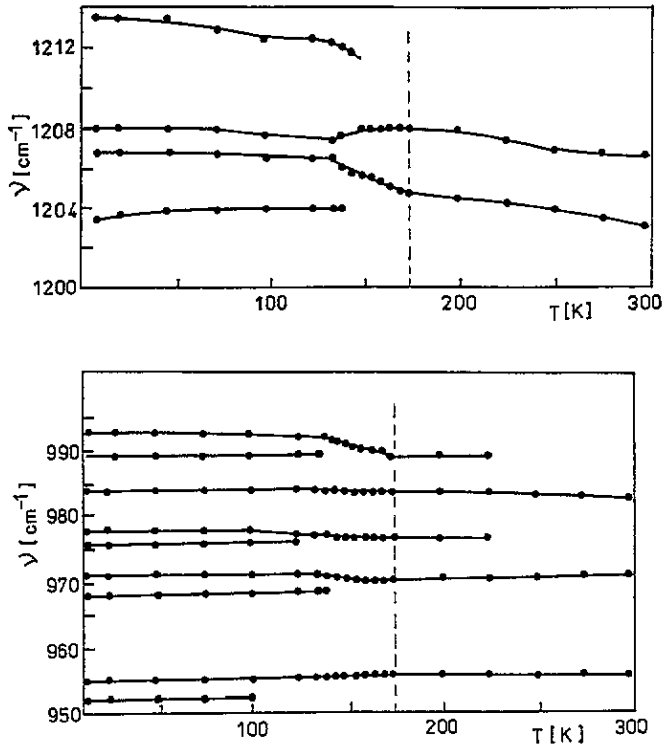

Figure 6. Temperature dependences of the frequencies for the $\rho(NM_3^+)$ mode and for the $\nu_a(CCC)$ (ν_{15}), ν(CN stretching) (ν_{13}) and $\rho(CH_3$ rocking) (ν_{29}) modes for IPBA crystal.

Table 4 contains the parameters of the relaxation process for the studied crystals: α is a parameter characterizing the distribution of relaxation times and $\Delta E^{\ddagger}$ is the value of activation energy.

4. Discussion

Preliminary x-ray diffraction studies show that isopropylammonium salts of the general formula $[(CH_3)_2CHNH_3]_2MX_5$ are isomorphous at room temperature. They are molecular-ionic salts. Compounds of R_2MX_5 stoichiometry crystallize with anionic sublattices built of either one-dimensional $(MX_5^{2-})_n$ chains composed of MX_6^{3-} octahedra sharing corners [16], isolated $M_2X_5^{4-}$ units composed of two octahedra sharing an edge [17], or isolated MX_5^{2-} square pyramidal units [18]. The cations are situated between anions connected to them by N–H···X hydrogen bonds. The structure of IPCB crystal was determined at room temperature and will be the subject of a separate work [19]. IPCB is monoclinic, space group $P2_1/c$. Its anionic sublattice is composed of isolated $Bi_2Cl_{10}^{4-}$ units. There are two crystallographically non-equivalent isopropylammonium cations in the crystal structure. One is ordered whereas the second one is disordered by splitting the position of the tertiary carbon atom between two sites with occupancy factor 0.5.

DSC and dilatometric studies reveal the existence of low-temperature structural phase transitions in a close temperature range, i.e. 150–180 K; however, the nature and sequences of these transformations are rather different. The characteristic feature of all phase transitions

Table 3. Wavenumbers (cm^{-1}), relative intensities[a] and tentative assignment of the IR bands arising from the internal vibrations of isopropylammonium cations in the IPBA crystal at 300 and 13 K.

$T = 300$ K	$T = 13$ K	Isopropylamine [15]	Tentative assignment
		3411	$\nu_a(NH_2)$ (ν_{20})
		3340	$\nu_s(NH_2)$ (ν_1)
3180s	3220s		
3121s	3121s		$\nu_a(NH_3^+)$
	3183m		
	3063vw		
3095s	3100s		$\nu_s(NH_3^+)$
	3076m		
3048s	3041m		
		2979	$\nu(CH_3)$ (ν_2)
2970m[b]	—	2968	$\nu(CH_3)$ (ν_3)
		2878	$\nu(CH_3)$ (ν_4)
2940vw[b]	—	2807	$\nu(CH)$ (ν_5)
		1622	$\delta(NH_2)$ (ν_6)
1591s	1606w		
1580s	1596m		
1567s	1567s		$\delta(NH_3^+)$
	1589w		
	1579s		
1476m[b]	—	1472	$\delta_d(CH_3)$ (ν_8)
		1462	$\delta_d(CH_3)$ (ν_{24})
1468m[b]	—	1380	$\delta_s(CH_3)$ (ν_9)
	—	1357	$\delta(CH)$ (ν_{26})
1380s[b]	—	1343	$\delta(CH)$ (ν_{10})
		1240	$\tau(CH_2)$ (ν_{27})
1356w[b]	—		
	1213w		
1207s	1208vw		
1203s	1207s		$\rho(NH_3^+)$
	1203w		
1155m	1155m	1175	$\rho(C)_3$) (ν_{11})
		1127	$\rho(CH_3)$ (ν_{12})
	993m		
983s	989w	1030	$\nu_a(CCC)$ (ν_{15})
	984s		
	978w		
971s	976vw		
	971s	978	$\nu(CN)$ (ν_{13})
	968m		
956w	955m	962	$\rho(CH_3)$ (ν_{29})
	952vw		
	937w		
932w	932vw		
	930m		$\omega(NH_3^+)$ (ν_{14})
922w	926s		
	919m		
796m	799s		
794m	796m	811	$\nu_s(CCC)$ (ν_{15})
	793s		

[a] vs, very strong; s, strong; m, medium; w, weak; v, very weak.
[b] Assignments for the spectrum of the pellet in KBr.

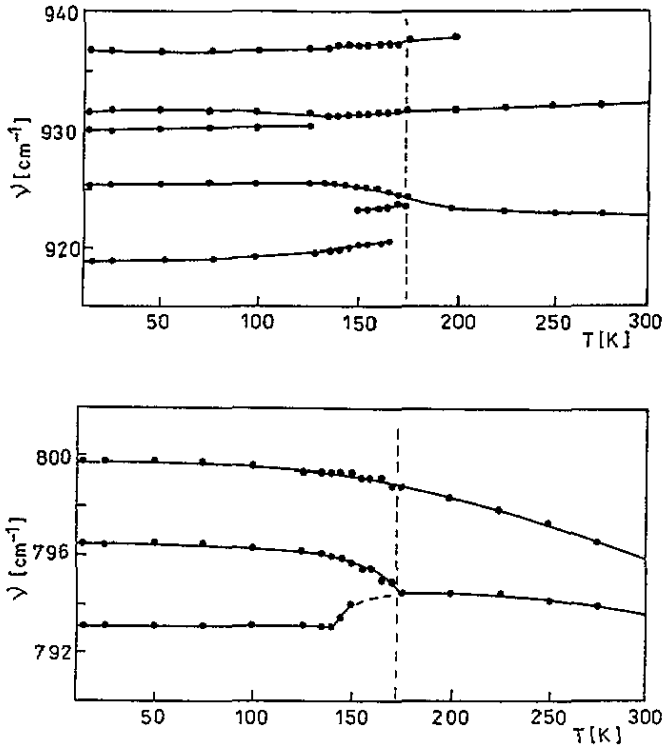

Figure 7. Temperature dependences of the $\omega(NH_3^+$ wagging) (ν_{14}) and ν_s(CCC) (ν_{15}) mode frequencies for IPBA crystal.

is relatively insignificant thermal anomalies both in the DSC curves and in thermal expansion. Thus we deal with a weak first- or higher-order phase transition. The entropy effects for the first-order transitions is found to be of the order of 1 J mol^{-1} K^{-1}. It indicates the insignificant change in the ordering and it is rather small as expected for the 'order–disorder' mechanism of these transitions.

All the studied isopropylammonium crystals show similar dielectric properties. Since the values of the permittivity are of the order of 15–10 units for the *b* and *c* directions, the *bc* plane seems to be distinguished for all studied crystals. On the other hand, along the *a* axis the observed values of ε' is two- to threefold lower. The maximum changes of dielectric increments $\Delta\varepsilon \simeq 2.5$–3 (when the phase transition point is approached from above) are observed in the cleavage (*bc*) plane of the crystal. Along the *a* axis, only the projection of the main dipole relaxator is visible. Such an anisotropy of dielectric properties suggests that the motion of the dielectrically active dipoles gives the basic contribution to the polarizability in the *bc* plane, in which the existence of the layer structure of the anionic sublattice is expected. Very recent x-ray studies [19] revealed that IPCB consists of $Bi_2Cl_{10}^{4-}$ anions sandwiched between isopropylammonium cations. These are attached to the layers via hydrogen bonds between NH_3^+ groups and chlorine ions. The adjacent layers, which are perpendicular to the *a* axis, are connected by van der Waals interactions of methyl groups of different isopropylammonium cations. In such a plane increased polarizability is usually observed and the dipole–dipole interactions are facilitated (similar to the other alkylammonium crystals [20, 21]).

For the crystals considered here striking similarities were found in the dynamic dielectric

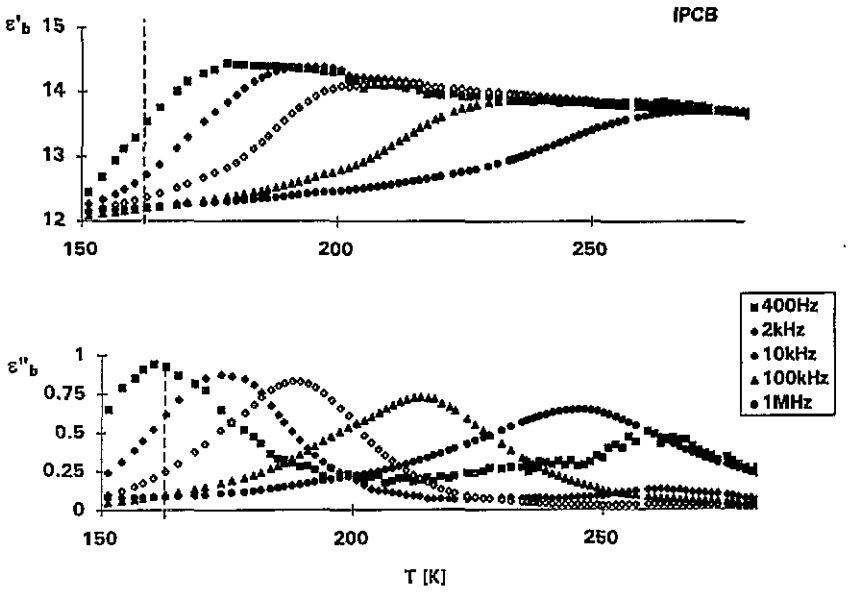

Figure 8. Temperature dependence of real (ε') and imaginary (ε'') parts of the permittivity for five frequencies between 400 Hz and 1 MHz along the *b* axis for IPCB crystal, on cooling. The vertical broken line represents the temperature of the phase transition taken from the dilatometric measurements (on cooling).

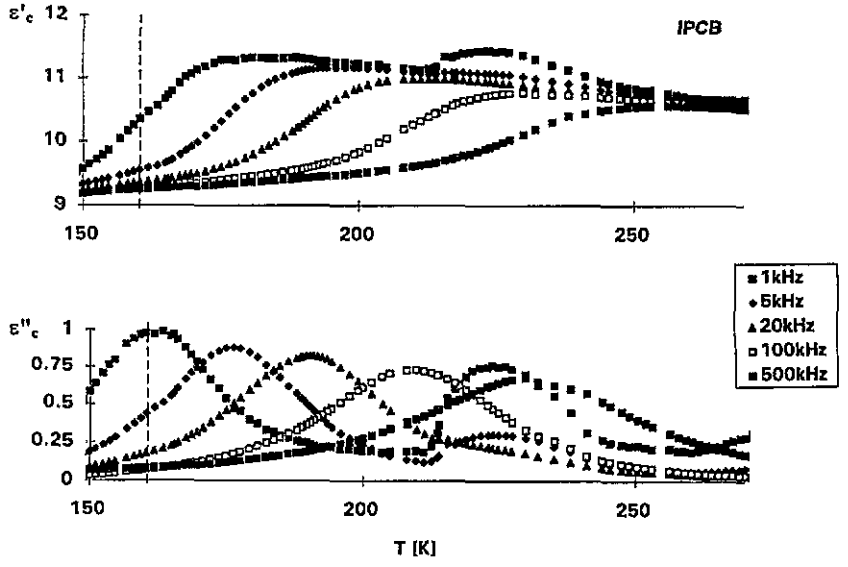

Figure 9. Temperature dependence of real (ε') and imaginary (ε'') parts of the permittivity for five fequencies between 400 Hz and 1 MHz along the *c* axis for IPCB crystal, on cooling.

behaviour, $\varepsilon^*(\omega, T)$ for the low-frequency region. The low-frequency relaxator that was found in the crystals under study is distinctly temperature-dependent and its macroscopic relaxation time is relatively long (of the order of 10^{-5}–10^{-4} s) in the vicinity of the phase

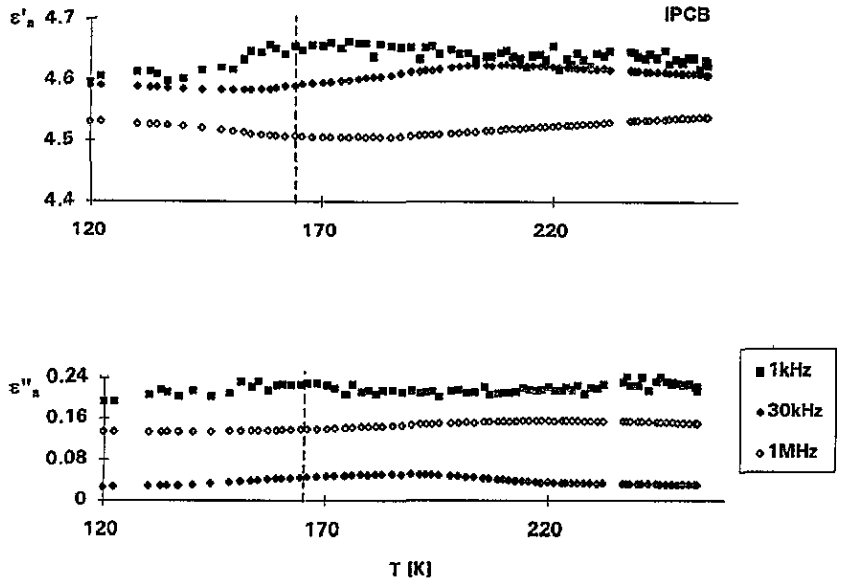

Figure 10. Temperature dependence of real (ε') and imaginary (ε'') parts of the permittivity for three frequencies between 400 Hz and 1 MHz along the a axis for IPCB crystal, on cooling.

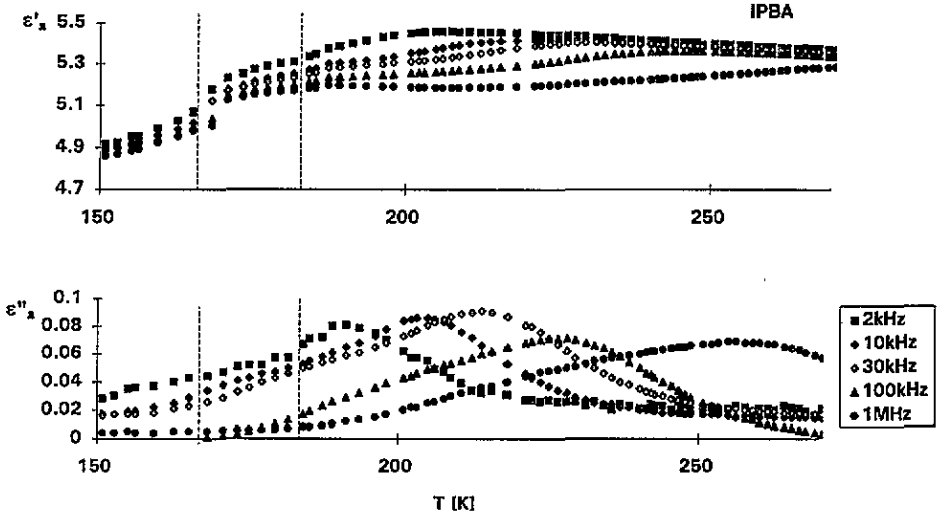

Figure 11. Temperature dependence of real (ε') and imaginary (ε'') parts of the permittivity for five frequencies between 400 Hz and 1 MHz along the a axis for IPBA crystal, on cooling.

transition temperatures. The estimated activation energies for the reorientational motion of the active dipole are comparable for all the crystals (~ 0.30 eV $= 4.32 \times 10^{-20}$ J). If the phase transitions are assumed to be connected with the release of the isopropylammonium cations, it is possible that more than one N–H$\cdots$X hydrogen bond is broken, which explains the high value of the activation energy. The dielectric results suggest also that we deal with a very slow anisotropic motion of dipole forms of the isopropylammonium cations as a

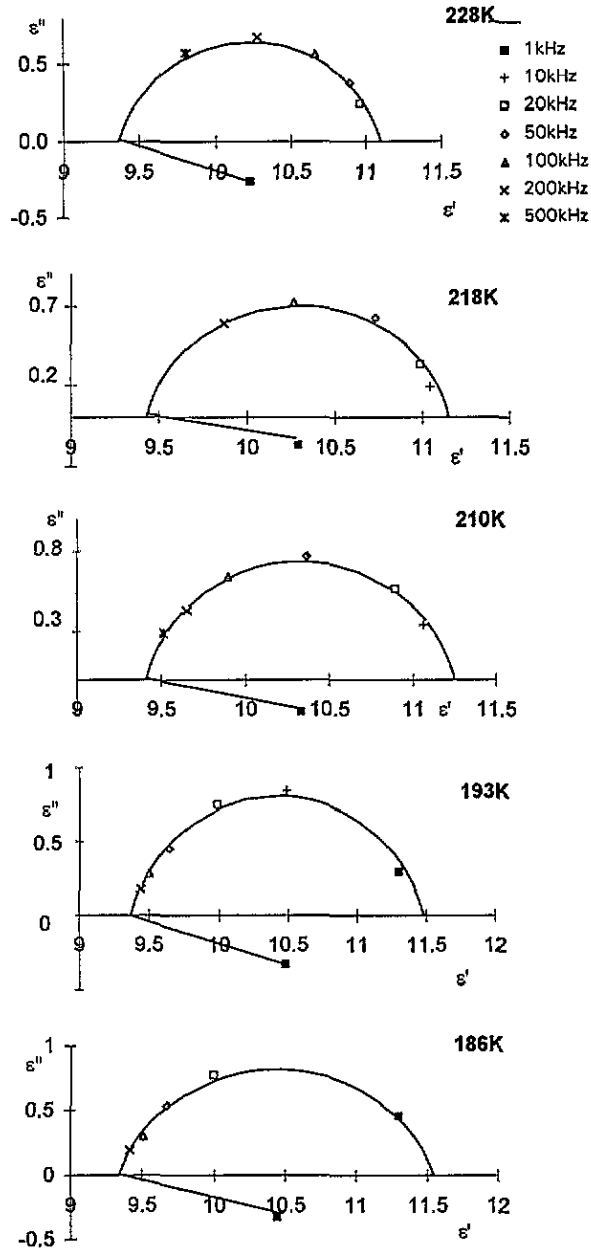

Figure 12. Cole–Cole diagrams at five temperatures (228, 218, 210, 193 and 186 K) for IPCB crystal.

whole. The phase transitions found are in the temperature region of dielectric dispersion. They may thus be connected with lattice instabilities caused by freezing of reorientation of isopropyl cations. The x-ray studies [19] corroborated the dynamical disorder of one of two non-equivalent isopropylammonium cations at room temperature.

The characteristic feature of the observed low-frequency dispersion is the distribution

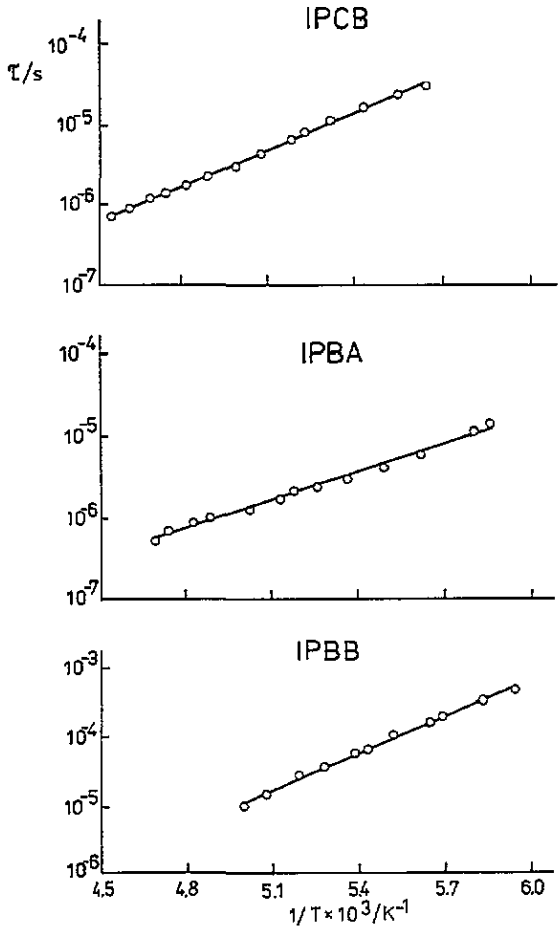

Figure 13. The $\log \tau$ versus $1/T$ plot for the IPCB, IPBA and IPBB crystals.

Table 4. Parameters of relaxation process for IPBB, IPCB and IPBA crystals in the high-temperature phase.

	T_c^a (K)	α	ΔE (eV)
IPCB	161	0.12–0.19	0.31
IPBA	167	0.19–0.24	0.27
IPBB	155	0.13–0.20	0.31

[a] T_c values taken on cooling, from the dilatometric studies.

of the relaxation times of the order of $\alpha \simeq 0.15$–0.2, independent of temperature. This phenomenon may have two reasons: the presence of defects or the existence of at least two relaxators with similar relaxation times. Both reasons are probable.

It was found that virgin samples of all derivatives that were cooled directly from room temperature showed distinct anomalies of ε' and ε'' in the temperature range 200–220 K. On the other hand, samples annealed at higher temperatures, after cooling, show only remnant dielectric anomalies in the same temperature range, which would confirm the defective mechanism of the anomalies mentioned above. It should be noted that the DSC and dilatometric studies did not reveal any distinct anomalies between 200 and 220 K.

The annealing of samples does not influence the distribution of the relaxation times at temperatures characteristic for dielectric dispersion.

The infrared studies of IPBA showed that only the ν_{15} and ν_{14} modes (C–C symmetric stretching and NH_3^+ wagging modes, respectively) of internal vibrations of the isopropylammonium cation exhibit weak temperature anomalies in the vicinity of the critical point ($T_c = 171$ K). It means that the changes in the dynamical state of the cation are very subtle. The distinct change in the IR spectra in the lower temperature region at about 140 K could suggest the sudden freezing of the C_3 reorientation of the CH_3 and NH_3 groups.

5. Conclusions

DSC and dilatometric studies of the $[(CH_3)_2CHNH_3]_2MX_5$ (M = Sb, B; X = Cl, Br) crystals reveal the existence of structural phase transitions, both first and higher order, in the low-temperature region.

Low-frequency dielectric relaxation described by the Cole–Cole equation is found in all the isopropylammonium derivatives in a similar temperature range.

Dielectric investigations confirm the existence of the structural phase transitions found by DSC and dilatometric techniques.

Dynamics of isopropylammonium cation gives a basic contribution to the mechanism of the phase transition of the 'order–disorder' type.

Temperature changes of the internal vibration modes of the isopropylammonium cation in IPBA crystal confirm its contribution to the phase transition mechanisms.

References

[1] Jakubas R and Sobczyk L 1990 *Phase Transitions* **20** 168
[2] Zaleski J, Jakubas R and Sobczyk L 1990 *Phase Transitions* **27** 25
[3] Varna V, Bhattarcharjee R, Vasan H N and Rao C N R 1992 *Spectrochim. Acta.* **48A** 1631
[4] Ishihara H, Watanabe K, Iwata A, Yamada K, Kinoshita Y, Okuda T, Krishnan V G, Dou S and Weiss A 1992 *Z. Naturf.* **47a** 65
[5] Jakubas R 1989 *Solid State Commun.* **69** 267
[6] Lefebvre J, Carpentier P and Jakubas R 1991 *Acta Crystallogr.* B **47** 228
[7] Whealy R D and Blackstock J B 1964 *J. Inorg. Nucl. Chem.* **26** 243
[8] Allen G C and McMeeking R F 1977 *J. Inorg. Chim. Acta* **23** 185
[9] Jagodziński P W and Laane J 1980 *J. Raman Spectrosc.* **9** 1
[10] Laane J and Jagodziński P W 1980 *Inorg. Chem.* **19** 44
[11] Okuda T, Kinoshita Y, Terao H and Yamada K 1994 *Z. Naturf.* **49a** 185
[12] Jakubas R, Bator G, Foulon M, Lefebvre J and Matuszewski J 1992 *Z. Naturf.* **48a** 529
[13] Piślewski N, Tritt-Goc J and Jakubas R 1994 *Solid State NMR* **3** 293
[14] Mitsui T, Tatsuzaki I and Nakamura E 1976 *An Introduction to the Physics of Ferroelectrics* (London: Gordon and Breach) ch V
[15] Hamada M 1988 *Chem. Phys.* **125** 55
[16] McPherson W G and Meyers E A 1968 *J. Phys. Chem.* **72** 553
[17] Lazarini F 1977 *Acta Crystallogr.* B **33** 1955
[18] Wismer R K and Jacobson R A 1974 *Inorg. Chem.* **13** 1679
[19] Zaleski J *et al* to be published
[20] Jakubas R, Czapla Z, Galewski Z and Sobczyk L 1986 *Ferroelectr. Lett.* **5** 143
[21] Gdaniec M, Kosturkiewicz Z, Jakubas R and Sobczyk L 1988 *Ferroelectrics* **77** 31